# Analysis of a compressed thin film bonded to a compliant substrate: the energy scaling law*

Robert V. Kohn† and Hoai-Minh Nguyen‡

*Revised version, Sept 9, 2012*
*Submitted to Journal of Nonlinear Science*

**Abstract**

We consider the deformation of a thin elastic film bonded to a thick compliant substrate, when the (compressive) misfit is far beyond critical. We take a variational viewpoint – focusing on the total elastic energy, i.e. the membrane and bending energy of the film plus the elastic energy of the substrate – viewing the buckling of the film as a problem of energy-driven pattern formation. We identify the scaling law of the minimum energy with respect to the physical parameters of the problem, and we prove that a herringbone pattern achieves the optimal scaling. These results complement previous numerical studies, which have shown that an optimized herringbone pattern has lower energy than a number of other patterns. Our results are different because (i) we make the scaling law achieved by the herringbone pattern explicit, and (ii) we give an elementary, ansatz-free proof that no pattern can achieve a better law.

## 1 Introduction

We study a variational problem modeling the deformation of a thin elastic film bonded to a thick, compliant substrate. When the (compressive) misfit is large enough the film buckles and complex, ordered structures are observed (see e.g. [8, 10, 11, 12, 22, 23, 30, 32, 34]). In the isotropic setting, a bifurcation analysis predicts a "checkerboard pattern" [1, 10] when the misfit is close to critical. For moderate misfits, there seem to be numerous patterns with similar energies. For large misfits it appears that a "herringbone" pattern (Figure 1) is preferred [10, 11, 12, 34], along with its disordered analogue, the "labyrinth" pattern [22, 23].

The behavior for moderate misfit has been studied by time-dependent numerical simulation [22, 23], by looking for secondary bifurcations [1, 2, 10, 32], and by comparing the energies of specific patterns [11, 12, 34]. Far from the bifurcation, however, it is natural to focus on the *scaling law* of the minimum energy, since different patterns should have different scaling laws [3].

*RVK gratefully acknowledges partial support from NSF grants DMS-0807347 and OISE-0967140.
†Courant Institute of Mathematical Sciences, New York University, kohn@cims.nyu.edu
‡Department of Mathematics, University of Minnesota, hmnguyen@math.umn.edu

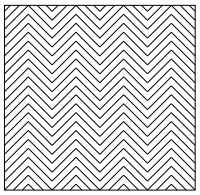

Figure 1: *Schematic representation of the herringbone pattern. The lines indicate extrema of the buckled film (they are not creases). Our analytical representation of the herringbone uses sinusoidal wrinkling. For experimental realizations see e.g. Figure 1 of [12], Figure 4 of [34], or Figure 2 of [30].*

The contribution of the present paper is two-fold:

(i) we identify the scaling law of the minimum energy, by proving upper and lower bounds that scale the same way, and

(ii) we "explain" the advantage of the herringbone pattern, by showing that it achieves the optimal scaling law.

These achievements are linked: the upper bound announced in (i) is proved using the herringbone pattern.

Our scaling-oriented viewpoint is similar to the one adopted by Audoly and Boudaoud in [3]. That paper considered several patterns, determining for each the associated scaling law. The one with the best law was a periodic "Miura-ori" folding pattern. Our analysis reveals that the Miura-ori pattern is *not* optimal; indeed, the herringbone pattern does better (see Section 1.4).

To identify the energy scaling law, it is crucial to prove a lower bound as well as an upper bound. Moreover, the lower bound must be ansatz-free, since it must apply to *any* pattern. The successful argument, which is surprisingly elementary, is presented in Section 2.

We are not the first to show that a herringbone structure has relatively low energy; this was previously shown numerically or semi-analytically in [10, 11, 12, 22, 34]. We are, however, the first to identify the energy scaling law associated with this structure, and to give an ansatz-free argument that it is optimal.

Our work adds to the list of energy-driven pattern formation problems where the scaling law of the minimum energy is known. Other examples involving wrinkling include blisters in compressed thin films [6, 7, 27], wrinkling in confined floating sheets [29], and wrinkling in a sheet under tensile loading [5]. Examples involving different physical systems include the intermediate state of a type-I superconductor [14], domains in a uniaxial ferromagnet [13], and twinning near an austenite-martensite interface [15, 28].

Our scaling-oriented viewpoint has advantages and disadvantages. A key advantage is that it permits rigorous analysis. A key disadvantage is that the configurations observed in experiments may be local rather than global energy minimizers. In fact, herringbone structures form mainly in systems where the preparation or elastic properties or patterning introduce some anisotropy; in a fully isotropic setting one typically sees a more disordered

"labyrinth" structure [8, 22, 23, 24, 25, 30, 38]. While the labyrinth structure looks like a disordered analogue of the herringbone pattern, we do not know whether it achieves the optimal scaling law (though there is numerical evidence that this is so [22]). Systems where the misfit is associated with a diffusive effect often form structures other than labyrinths and herringbones, see e.g. [9, 33, 37]; perhaps the diffusive kinetics introduces a different notion of "local minimum."

A key feature of our approach is its focus on the scaling law (not the prefactor). As a result, our conclusions are compelling only for systems where the compressive stress is far beyond critical – the "far from threshold" regime, in the language of [17].

The problem studied here is part of a larger literature on the origins and applications of wrinkling patterns in thin elastic films. For recent reviews see [20, 36], and (for a broader, more theoretical perspective) [4].

### 1.1 The model

Our framework is very similar to those of prior analyses such as [1, 2, 3, 11, 12, 22, 23, 34], so the discussion of the model can be relatively brief. We use von Karman plate theory, for a film of thickness $h$. To facilitate spatial averaging, the system is assumed to be periodic with periodicity $L$ in both directions (but our energy scaling law will depend on $L$ only through the nondimensionalized thickness $h/L$). We work with the (normalized) energy per unit area

$$\mathcal{E} = \mathcal{E}_m + \mathcal{E}_b + \mathcal{E}_s \tag{1}$$

where

$$\mathcal{E}_m = \frac{\alpha_m h}{L^2} \int_{[0,L]^2} \left| e(w) + \tfrac{1}{2} \nabla u_3 \otimes \nabla u_3 - \eta I \right|^2, \tag{2}$$

is the *membrane term*,

$$\mathcal{E}_b = \frac{h^3}{L^2} \int_{[0,L]^2} |\nabla^2 u_3|^2 \tag{3}$$

is the *bending term*, and

$$\mathcal{E}_s = \frac{\alpha_s}{L^2} \|u_3\|^2_{H^{1/2}}, \tag{4}$$

is the *substrate term*. Here $w = (w_1, w_2)$ is the in-plane displacement of the film; $u_3$ is the out-of-plane displacement; $e(w) = \frac{1}{2}(Dw + Dw^T)$ is the linear strain associated with $w$; and $\nabla u_3 \otimes \nabla u_3$ is the rank-one $2 \times 2$ matrix $(\nabla u_3)(\nabla u_3)^T$. The misfit $\eta$ is assumed positive (so the film, if undeformed, is compressed by the substrate) and small (so von Karman theory is appropriate). Notice that there is no elastic modulus in front of $\mathcal{E}_b$; thus, $\mathcal{E}$ has already been normalized by the stiffness of the film, and it has the dimensions of length.

Since our goal is a scaling law (not the prefactor) there is no need to keep constants of order one; in particular, our use of a Hooke's law with Poisson's ratio zero in the membrane term represents no loss of generality. It is tempting, by the same logic, to set $\alpha_m = 1$, since von Karman plate theory assigns it a value of order 1. But we will soon rescale the problem, and our rescaling changes the constant in front of the membrane term (see Section 1.3). Therefore we prefer to keep $\alpha_m$ explicit.

Our notation in (4) is that if $u_3(x) = \sum_\xi e^{i\xi\cdot x}\hat{u}_3(\xi)$ then

$$\|u_3\|^2_{H^{1/2}} = \sum_\xi |\xi||\hat{u}_3|^2(\xi). \tag{5}$$

(Lest there be any confusion please note: we are using the notation $\|\cdot\|_{H^{1/2}}$ for the *homogeneous* $H^{1/2}$ norm.) The nonlocal term $\mathcal{E}_s$ represents the normalized elastic energy of the substrate; in particular, the dimensionless constant $\alpha_s$ in (4) is the stiffness of the substrate divided by the stiffness of the film.

One might ask why the substrate term $\mathcal{E}_s$ involves only $u_3$, not the in-plane displacement $w$. This modeling hypothesis is discussed e.g. in [1]; briefly, the logic is that within von Karman theory the in-plane displacements are much smaller than the out-of-plane displacements, so the substrate energy associated with $w$ should be negligible. Actually, this argument is only partly correct: it gets the scaling law of the minimum energy right (if the misfit $\eta$ is sufficiently small, see (13)), but it does not fully explain the herringbone pattern. Indeed, the pattern has two well-separated length scales. The smaller one – the wavelength of the wrinkling – is predicted unambiguously by the framework summarized above. But this framework leaves the larger one – the scale on which the wrinkling direction oscillates – ambiguous [12, 22, 34].

To do better, one must keep the substrate energy associated with $w$ (as already noted in [22]). Therefore in Section 4 we consider the improved model

$$\mathcal{E}^* = \mathcal{E}_m + \mathcal{E}_b + \mathcal{E}^*_s \tag{6}$$

where $\mathcal{E}_m$ and $\mathcal{E}_b$ are as before and

$$\mathcal{E}^*_s = \frac{\alpha_s}{L^2}\left(\|u_3\|^2_{H^{1/2}} + \|w\|^2_{H^{1/2}}\right). \tag{7}$$

While the inclusion of the substrate energy[1] due to $w$ does not change the energy scaling law (if the misfit is sufficiently small), we'll show that it gives a preferred value for the scale on which the wrinkling direction oscillates. But this preferred value comes from optimizing a subdominant energy (see Remark 3), so getting the value right is not energetically essential. This is consistent with the numerical and experimental observation that while the length scale of the wrinkling is sharply determined, the scale on which the wrinkling oscillates is much less sharply determined [12, 22, 34].

In practice the displacement $(w_1, w_2, u_3)$ should have mean value 0. This is implicit in the model, since otherwise the elastic energy of substrate would be infinite (if the substrate is semi-infinite). However it is irrelevant to the mathematics, since the energies $\mathcal{E}$ and $\mathcal{E}^*$ are unchanged when we subtract the mean displacement. Therefore we may safely ignore the condition of having mean value 0 in our analysis of the energy.

[1] In giving the substrate energies of $u_3$ and $w$ the same weight in (7) we have ignored a constant of order one; as discussed earlier, this is appropriate since we seek only the energy scaling law.

### 1.2 Main results

We are interested in how the minimum of $\mathcal{E}$ or $\mathcal{E}^*$ depends on $h$ and $L$ (which have the dimensions of length) and $\eta$, $\alpha_m$, $\alpha_s$ (which are dimensionless). Our main results concerning $\mathcal{E}$ are the following:

**Theorem 1** (Lower Bound)**.** *There is a constant $C_1$, independent of all the parameters, such that*

$$\min \mathcal{E} \geq C_1 \min \left\{ \alpha_m \eta^2 h, \alpha_s^{2/3} \eta h \right\}. \tag{8}$$

**Theorem 2** (Upper bound)**.** *There is a constant $C_2$, independent of all the parameters, such that if either*

$$\alpha_m \eta \leq \alpha_s^{2/3} \tag{9}$$

*or*

$$\alpha_m \eta \alpha_s^{-1} \frac{h}{L} \leq 1 \tag{10}$$

*then*

$$\min \mathcal{E} \leq C_2 \min \left\{ \alpha_m \eta^2 h, \alpha_s^{2/3} \eta h \right\}. \tag{11}$$

*When (9) holds the assertion is trivial: it suffices to consider $(w_1, w_2, u_3) = 0$. When (9) fails and (10) holds, the proof uses a version of the herringbone pattern, with wrinkling on a length scale of order $\alpha_s^{-1/3} h$.*

The case of primary interest is when $\alpha_s^{2/3} \ll \alpha_m \eta$ and $h/L$ is sufficiently small. In this far-beyond-critical setting, the theorems combine to show that the energy scaling law is $\min \mathcal{E} \sim \alpha_s^{2/3} \eta h$.

Turning now to $\mathcal{E}^*$: we shall show that if $\eta$ is small enough then $\mathcal{E}^*$ has the same scaling law as $\mathcal{E}$; moreover, the proof indicates the scale on which the wrinkling direction should oscillate in the herringbone pattern. Our main result is:

**Theorem 3** (The improved model)**.** *Since $\mathcal{E}^* \geq \mathcal{E}$, the lower bound (8) applies to $\mathcal{E}^*$ as well as $\mathcal{E}$. Concerning the upper bound: there is a constant $C_3$, independent of all the parameters, such that if either*

$$\alpha_m \eta \leq \alpha_s^{2/3} \tag{12}$$

*or else*

$$\alpha_m \alpha_s^{-4/3} \left( \frac{h}{L} \right)^2 \leq 1 \quad \text{and} \quad \eta^2 \leq \alpha_m^{-1} \alpha_s^{2/3} \tag{13}$$

*we have*

$$\min \mathcal{E}^* \leq C_3 \min \left\{ \alpha_m \eta^2 h, \alpha_s^{2/3} \eta h \right\}. \tag{14}$$

*When (12) fails and (13) holds, the proof uses a version of the herringbone pattern, with wrinkles on scale $a_0 \sim \alpha_s^{-1/3} h$ whose direction oscillates on the longer scale $\alpha_m^{1/2} \eta^{-1/2} \alpha_s^{-1/3} a_0$.*

Theorem 3 shows, in particular, that if $\alpha_m$ and $\alpha_s$ are held fixed and $\eta$ satisfies a smallness condition (depending only on $\alpha_s$ and $\alpha_m$), then $\min \mathcal{E} \sim \min \mathcal{E}^* \sim \min \left\{ \alpha_m \eta^2 h, \alpha_s^{2/3} \eta h \right\}$ provided $h/L$ is sufficiently small.

Theorem 1–3 will be proved in Sections 2–4 respectively. Each section begins with a brief summary of the main idea.

### 1.3 Reduction to $L = 1$ and $\eta = 1$

The reduction to $L = 1$ is a matter of nondimensionalization. The reduction to $\eta = 1$ uses the special form of the von Karman energy, and is restricted to $\mathcal{E}$ (though something similar can be done for $\mathcal{E}^*$, c.f. (42)). Doing both reductions at once: let us define $(\tilde{w}_1, \tilde{w}_2, \tilde{u}_3)$ by

$$w(x, y) = \eta L \tilde{w}(x/L, y/L), \quad u_3(x, y) = \sqrt{\eta} L \tilde{u}_3(x/L, y/L) \tag{15}$$

so that $w$ and $u_3$ are periodic with period 1, and

$$\tilde{\alpha}_m = \alpha_m \eta, \quad \tilde{h} = h/L.$$

Then (by mere algebra, starting from (1)) one verifies that

$$\mathcal{E} = \eta L \left\{ \tilde{\alpha}_m \tilde{h} \int_{[0,1]^2} \left| e(\tilde{w}) + \tfrac{1}{2} \nabla \tilde{u}_3 \otimes \nabla \tilde{u}_3 - I \right|^2 + \tilde{h}^3 \int_{[0,1]^2} |\nabla^2 \tilde{u}_3|^2 + \alpha_s \|\tilde{u}_3\|^2_{H^{1/2}} \right\}. \tag{16}$$

The expression in brackets is our functional $\mathcal{E}$ with $L$ replaced by 1, $\eta$ replaced by 1, $h$ replaced by $\tilde{h}$, and $\alpha_m$ replaced by $\tilde{\alpha}_m$. It follows readily that if Theorems 1 and 2 hold when $L = 1, \eta = 1$ then they hold for all $L$ and $\eta$. (Lest there be any confusion: in the original physical variables, $h$ is the thickness of the film and the period cell has size $L$. When we apply Theorem 2 in the reduced variables, the wrinkles have scale $\alpha_s^{-1/3}\tilde{h}$ in the nondimensionalized spatial variables $(x/L, y/L)$. Therefore the physical scale of the wrinkling is $\alpha_s^{-1/3}\tilde{h}L = \alpha_s^{-1/3}h$, as asserted by the theorem.

### 1.4 Perspective

The paper [3] studies several patterns, identifying the scaling law of each. The one with the best scaling law (the largest exponent of $\alpha_s$) is the origami-inspired "Miura-ori" construction[2] (see Figure 2), which achieves (in our notation) $\mathcal{E} \sim \alpha_m^{1/16} \alpha_s^{5/8} \eta^{17/16} h$. Since the trivial deformation $w = 0, u_3 = 0$ is always a possibility, their argument shows that if $h/L$ is sufficiently small then

$$\min \mathcal{E} \leq C \min \left\{ \alpha_m \eta^2 h, \alpha_m^{1/16} \alpha_s^{5/8} \eta^{17/16} h \right\}. \tag{17}$$

Theorem 2 shows that while (17) is true, it is not optimal. Indeed, our herringbone pattern does better since $\alpha_m^{1/16} \alpha_s^{5/8} \eta^{17/16} > \alpha_s^{2/3} \eta$ when $\alpha_m \eta > \alpha_s^{2/3}$. We conclude, in particular, that the Miura-ori pattern is quite distinct from the herringbone. Physically: the Miura-ori structure has a lattice of creases in which both the bending and membrane energies are significant; therefore its scaling law depends on $\alpha_m$. In the herringbone pattern, by contrast, the membrane energy is identically zero except in the transition layers where the direction of wrinkling changes; since there are few such layers, the membrane energy (though not identically zero) is subdominant, and the energy scaling law is independent of $\alpha_m$.

[2]The paper [3] proposes the Miura-ori construction as a model for the herringbone pattern in the far-from-critical regime; in particular, it does not differentiate between the two. In our view, however, a key difference is that the Miura-ori construction involves sharp creases, while the herringbone pattern involves smooth wrinkles.

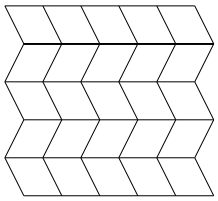

Figure 2: *Creases in the Miura-ori construction. Here (unlike Figure 1) the lines show the locations of creases in the unbuckled film. After buckling the image of each parallelogram is planar.*

Our lower bound assures that no pattern can have an energy scaling law better than that of the herringbone. It remains an open question, however, whether there are patterns other than the herringbone that achieve the same scaling. (In other words: we do not know whether there are wrinkling patterns entirely different from our herringbones, which also satisfy $\mathcal{E} \leq C\alpha_s^{2/3}\eta h$ or $\mathcal{E}^* \leq C\alpha_s^{2/3}\eta h$ when $\alpha_s^{2/3} \ll \alpha_m\eta$, under conditions analogous to (10) or (13).)

We describe our results as giving the "scaling law" of the minimum energy, because they bound it up to prefactors which are independent of all the parameters ($\alpha_m, \alpha_s, \eta, h$ and $L$). Our results are not restricted to an asymptotic regime; rather, they apply whenever the parameters satisfy certain inequalities. However since the upper and lower bounds have different prefactors, they are most informative in the "far from threshold" regime when $\alpha_s^{2/3} \ll \alpha_m\eta$. For example, it is only in this regime that our results rule out a lower bound analogous to (17) (i.e. a bound of the form $\min \mathcal{E} \geq C \min\left\{\alpha_m\eta^2 h, \alpha_m^{1/16}\alpha_s^{5/8}\eta^{17/16}h\right\}$).

This paper focuses on the case when the misfit is isotropic. Films with anisotropic misfit have been studied both experimentally and theoretically, see e.g. [25] and [41]. Our lower bound has an obvious extension to the anisotropic setting; it would be interesting to know the circumstances under which the resulting bound gives the optimal scaling law.

Our model uses von Karman plate theory. The von Karman approximation can be given a rigorous justification in some settings, see e.g. [19]. We wonder whether it can be justified in the present setting. There are some systems where the patterns involve large slopes (so the von Karman approximation is not appropriate) or the strains are large (so linear elasticity is inadequate for modeling the substrate), see e.g. [18, 35]. We wonder whether parts of our analysis might extend to a more fully nonlinear model.

Our model assumes that the film remains bonded to the substrate. There are systems where elastic misfit induces the nucleation and spreading of blisters, see e.g. [21, 26]. We wonder whether such blistering can be understood using an energy-based approach similar to that of the present paper. So far, analysis has been restricted to the case where the blistered region is known in advance and the substrate is rigid [6, 7, 27].

Taken together, Theorems 1 and 2 show that the herringbone comes within a constant of the minimum energy when the substrate is sufficiently compliant ($\alpha_s^{2/3} \ll \alpha_m\eta$) and the film is sufficiently thin ($h/L \leq \alpha_s(\alpha_m\eta)^{-1}$). When $\alpha_s = 0$ this conclusion is vacuous, since the "thinness" condition would then require $h/L = 0$. Our functional with $\alpha_s = 0$ is, however, still interesting, since it describes the spatially periodic "crumpling" of an

elastic sheet (in the small-slope regime, modelled using von Karman theory). An extensive literature has developed concerning the crumpling of elastic sheets [40], and the associated formation of singularities such as "ridges" [16, 31, 39]. It seems plausible that the Miura-ori construction discussed in [3, 32] might achieve the optimal scaling when $\alpha_s = 0$, however the lower bound implicit in this conjecture remains an intriguing open question.

## 2 Proof of the lower bound

This section presents the proof of Theorem 1. As explained in Section 1.3, it suffices to consider the case when $L = 1$ and $\eta = 1$. Therefore our goal is to show that if $u_3$ and $w$ are periodic with period 1, then[3]

$$\alpha_m h \int_{[0,1]^2} |e(w) + \tfrac{1}{2}\nabla u_3 \otimes \nabla u_3 - I|^2 + h^3 \int_{[0,1]^2} |\nabla^2 u_3|^2 + \alpha_s \|u_3\|_{H^{1/2}}^2 \gtrsim \min\left\{\alpha_m h, \alpha_s^{2/3} h\right\}. \tag{18}$$

The argument is simple in concept. There are two cases:

(i) If $\int |\nabla u_3|^2$ is small, then (as we'll see) the membrane term is nearly $\alpha_m h$ times $\int |e(w) - I|^2$. Since $w$ is periodic, the integral is bounded away from 0, so the membrane term cannot be too small.

(ii) If $\int |\nabla u_3|^2$ is large, then the interpolation inequality

$$\|\nabla u_3\|_{L^2} \lesssim \|\nabla^2 u_3\|_{L^2}^{1/3} \|u_3\|_{H^{1/2}}^{2/3} \tag{19}$$

(easily proved for any periodic function using the Fourier transform) shows that the bending and substrate terms cannot both be small.

Either way, the total energy cannot be too small.

*Proof of Theorem 1.* As noted above, we have only to prove (18). Since $w_2$ is periodic, $\int_{[0,1]^2} \partial_y w_2 = 0$. Therefore, using Jensen's inequality in the form $\left(\int_{[0,1]^2} f\right)^2 \le \int_{[0,1]^2} f^2$, we have

$$\int_{[0,1]^2} \Big[\partial_y w_2 + \tfrac{1}{2}|\partial_y u_3|^2 - 1\Big]^2 \ge \Big[\int_{[0,1]^2} \tfrac{1}{2}|\partial_y u_3|^2 - 1\Big]^2.$$

So it suffices to show that

$$\alpha_m h \Big[\int_{[0,1]^2} \tfrac{1}{2}|\partial_y u_3|^2 - 1\Big]^2 + h^3 \int_{[0,1]^2} |\nabla^2 u_3|^2 + \alpha_s \|u_3\|_{H^{1/2}}^2 \gtrsim \min\left\{\alpha_m h, \alpha_s^{\frac{2}{3}} h\right\}. \tag{20}$$

Let $c_0$ be a constant between 0 and 1 (for example, $c_0 = 1/2$ would be convenient). If

$$\Big[\int_{[0,1]^2} \tfrac{1}{2}|\partial_y u_3|^2 - 1\Big]^2 \ge c_0$$

[3]Here and in the rest of the paper, $a \gtrsim b$ means $a \ge Cb$ for some positive universal constant $C$. Similarly, $a \lesssim b$ means that $a \le Cb$ for some constant $C$, and $a \sim b$ means $a \lesssim b$ and $b \lesssim a$.

then the validity of (20) is obvious. Otherwise we have

$$\Big[\int_{[0,1]^2} \tfrac{1}{2}|\partial_y u_3|^2 - 1\Big]^2 < c_0,$$

whence

$$\begin{aligned}\frac{1}{2}\int_{[0,1]^2} |\nabla u_3|^2 &\geq 1 + \int_{[0,1]^2} \big(\tfrac{1}{2}|\partial_y u_3|^2 - 1\big) \\ &\geq 1 - c_0^{1/2} \\ &\gtrsim 1.\end{aligned}$$

We conclude using the interpolation inequality (19) that

$$\|\nabla^2 u_3\|_{L^2}^{1/3} \|u_3\|_{H^{\frac{1}{2}}}^{2/3} \gtrsim 1.$$

Therefore

$$\begin{aligned}h^3\|\nabla^2 u_3\|_{L^2}^2 + \alpha_s\|u_3\|_{H^{1/2}}^2 &= h^3\|\nabla^2 u_3\|_{L^2}^2 + \tfrac{1}{2}\alpha_s\|u_3\|_{H^{1/2}}^2 + \tfrac{1}{2}\alpha_s\|u_3\|_{H^{1/2}}^2 \\ &\gtrsim \Big(h^3\|\nabla^2 u_3\|_{L^2}^2\alpha_s^2\|u_3\|_{H^{1/2}}^4\Big)^{1/3} \\ &\gtrsim h\alpha_s^{2/3}\end{aligned}$$

using the arithmetic mean – geometric mean inequality in the second line. So the desired inequality (20) is valid, and the proof is complete. □

**Remark 1.** *In stating Theorem 1 we assumed that $w$ was periodic in both variables. But the proof uses much less: the only property of $w$ that we used was $\int \partial_y w_2 = 0$, which is true for example if $w_2$ is periodic only in $y$. A symmetric argument would work if $\int \partial_x w_1 = 0$, which is true for example if $w_1$ is periodic only in $x$. We used the periodicity of $u_3$ in both directions, however, to define the substrate energy $\mathcal{E}_s$ and to justify the interpolation inequality (19).*

# 3 Proof of the upper bound

This section presents the proof of Theorem 2. As explained in Section 1.3, it suffices to consider the case when $L = 1$ and $\eta = 1$. If $\alpha_m \leq \alpha_s^{2/3}$ the result is obvious, using $(w_1, w_2, u_3) = 0$. Therefore our task is to show that if

$$\alpha_s^{2/3} \leq \alpha_m \tag{21}$$

and if $h$ satisfies

$$\alpha_m \alpha_s^{-1} h \leq 1 \tag{22}$$

then a version of the herringbone pattern (using wrinkling on scale $\alpha_s^{-1/3}h$) achieves

$$\alpha_m h \int_{[0,1]^2} |e(w) + \tfrac{1}{2}\nabla u_3 \otimes \nabla u_3 - I|^2 + h^3 \int_{[0,1]^2} |\nabla^2 u_3|^2 + \alpha_s \|u_3\|^2_{H^{1/2}} \lesssim \alpha_s^{2/3} h. \quad (23)$$

The basic idea[4] is this: in the left half of the period cell we use straight wrinkles perpendicular to $(1,1)$ with wavelength $a_0$, superimposed on an in-plane shear of order 1. This can be done in such a way that the membrane term vanishes identically: $e(w) + \frac{1}{2}\nabla u_3 \otimes \nabla u_3 - I = 0$. In the right half of the period cell we use a similar (actually, mirror-image) construction, with straight wrinkles perpendicular to $(-1,1)$. This can be done in such a way that $(w_1, w_2, u_3)$ are continuous and periodic. There is a "boundary layer" in the middle, where the two families of wrinkles meet; the condition (22) will assure that its contribution to the energy is negligible. The length scale of the wrinkling is selected by optimizing the bending and substrate terms, which are of order $h^3 a_0^{-2}$ and $\alpha_s a_0$ respectively, leading to $a_0 \sim h\alpha_s^{-1/3}$. Since (21) and (22) combine to give

$$h\alpha_s^{-1/3} \leq 1, \quad (24)$$

the scale of the wrinkling is not larger than that of the period cell.

Like any herringbone pattern, this construction has two length scales: the scale of the wrinkling (of order $h\alpha_s^{-1/3}$) and the scale of the superimposed in-plane shear (of order 1). The former is physical, while the latter is not. Indeed, the scale on which the superimposed in-plane shear oscillates should be selected by a substrate term associated with $w$, which the functional $\mathcal{E}$ omits. We will do better in Section 4, by considering $\mathcal{E}^*$ rather than $\mathcal{E}$.

The idea at the heart of our construction – the fact that the one-dimensional wrinkling superimposed on an in-plane shear can make the membrane term vanish identically – goes back (at least) to the work of Jin & Sternberg and Ben Belgacem, Conti, DeSimone & Müller on blisters in compressed thin films [6, 27].

*Proof of Theorem 2.* As noted above, we need only show that if (21) and (22) hold, then there exist $(w_1, w_2, u_3)$ (periodic in both variables with period 1) such that (23) holds. The argument will be presented in several steps:

Step 1: Specify $(w_1, w_2, u_3)$ in $[0, 1/2] \times [0, 1]$.

Step 2: Estimate the membrane energy in $[0, 1/2] \times [0, 1]$.

Step 3: Estimate the bending energy in $[0, 1/2] \times [0, 1]$.

Step 4: Estimate the $L^2$-norms of $u_3$ and $\nabla u_3$ in $[0, 1/2] \times [0, 1]$.

Step 5: Specify $(w_1, w_2, u_3)$ in $[1/2, 1] \times [0, 1]$ and derive the conclusion.

[4]The summary presented here focuses on the rescaled problem, with misfit $\eta = 1$. For a brief summary using the original variables see Remark 2 at the end of this section.

Step 1: Fix $0 < a_0 \leq 1$ such that

$$a_0 \sim h\alpha_s^{-1/3} \quad \text{and} \quad \frac{1}{a_0} \in \pi\mathbb{N}_+. \tag{25}$$

Such an $a_0$ exists by (24). We define

$$\Omega_{1,\delta} = \big([0,\delta] \cup [1/2-\delta, 1]\big) \times [0,1] \quad \text{and} \quad \Omega_{2,\delta} = [\delta, 1/2-\delta] \times [0,1],$$

where $\delta$ is a small positive number such that

$$a_0 \lesssim \delta \lesssim \alpha_s^{2/3}\alpha_m^{-1}. \tag{26}$$

Such a $\delta$ exists by (22).

We choose $(w_1, w_2, u_3)$ on $\Omega_{2,\delta}$ as follows:

$$w_1(x,y) = \frac{a_0}{4}\sin\Big(\frac{4(x+y)}{a_0}\Big), \tag{27}$$

$$w_2(x,y) = \frac{a_0}{4}\sin\Big(\frac{4(x+y)}{a_0}\Big) - 2x, \tag{28}$$

and

$$u_3(x,y) = a_0\cos\Big(\frac{2(x+y)}{a_0}\Big). \tag{29}$$

To extend this deformation to $\Omega_{1,\delta}$, we use a smooth "cutoff function" $\varphi_\delta$ such that

$$\begin{aligned} \varphi_\delta(x) &= 0 \quad \text{for } x \leq \tfrac{1}{4}\delta \\ \varphi_\delta(x) &= 1 \quad \text{for } \tfrac{3}{4}\delta < x < \tfrac{1}{2} - \tfrac{3}{4}\delta \\ \varphi_\delta(x) &= 0 \quad \text{for } \tfrac{1}{2} - \tfrac{1}{4}\delta < x < \tfrac{1}{2} \end{aligned}$$

and

$$|\varphi_\delta| \lesssim 1, \quad |\varphi_\delta'| \lesssim \delta^{-1}, \quad |\varphi_\delta''| \lesssim \delta^{-2}.$$

(Such a function can, for example, be obtained by taking

$$\varphi_\delta(x) = \begin{cases} \psi(x/\delta) & \text{for } x \leq \delta \\ 1 & \text{for } \delta \leq x \leq \frac{1}{2} - \delta \\ \psi([\frac{1}{2} - x]/\delta) & \text{for } \frac{1}{2} - \delta \leq x \leq \frac{1}{2} \end{cases}$$

with $\psi$ chosen so that $\psi(x) = 0$ for $x \leq 1/4$ and $\psi(x) = 1$ for $x \geq 3/4$.) Our extension of the definition to $\Omega_{1,\delta}$ is now given by

$$w_1(x,y) = \frac{a_0}{4}\varphi_\delta(x)\sin\Big(\frac{4(x+y)}{a_0}\Big),$$

$$w_2(x,y) = \frac{a_0}{4}\varphi_\delta(x)\sin\Big(\frac{4(x+y)}{a_0}\Big) - 2x,$$

and

$$u_3(x,y) = a_0\varphi_\delta(x)\cos\Big(\frac{2(x+y)}{a_0}\Big);$$

these formulas apply for *all* $x \in [0,1/2]$, since they reduce to (27)–(29) when $\delta \le x \le 1/2-\delta$. Clearly

$$u_3(0,y) = u_3(1/2,y) = 0, \quad \nabla u_3(0,y) = \nabla u_3(1/2,y) = (0,0), \quad w_1(0,y) = w_1(1/2,y) = 0,$$

while

$$w_2(0,y) = 0, \quad \text{and} \quad w_2(1/2,y) = -1.$$

We also have

$$|\nabla u_3| + |\nabla w_1| + |\nabla w_2| \lesssim 1 \quad \text{and} \quad |\nabla^2 u_3| \lesssim 1/a_0 \tag{30}$$

in $[0,1/2]\times[0,1]$. (We use here the fact that $a_0 \lesssim \delta$.)

Step 2: The membrane energy on $[0,1/2]\times[0,1]$ is

$$\alpha_m h \int_0^{1/2}\int_0^1 \Big|e(w_1,w_2) + \tfrac{1}{2}\nabla u_3\otimes\nabla u_3 - I\Big|^2.$$

From (29), we have

$$\partial_y u_3 = -2\sin\Big(\frac{2(x+y)}{a_0}\Big) \quad \text{in } \Omega_{2,\delta}, \tag{31}$$

which implies

$$\frac{1}{2}|\partial_y u_3|^2 = 2\sin^2\Big(\frac{2(x+y)}{a_0}\Big) \quad \text{in } \Omega_{2,\delta}. \tag{32}$$

On the other hand, from (28) we obtain

$$\partial_y w_2 = \cos\Big(\frac{4(x+y)}{a_0}\Big) \quad \text{in } \Omega_{2,\delta}. \tag{33}$$

A combination of (32) and (33) yields

$$\partial_y w_2 + \frac{|\partial_y u_3|^2}{2} - 1 = 0 \quad \text{in } \Omega_{2,\delta}. \tag{34}$$

Since

$$\partial_x w_1 = \partial_y w_1 = \partial_y w_2 = \partial_x w_2 + 2 \quad \text{and} \quad \partial_x u_3 = \partial_y u_3 \quad \text{in } \Omega_{2,\delta},$$

it follows from (34) that

$$\partial_x w_1 + \frac{|\partial_x u_3|^2}{2} - 1 = 0 \quad \text{and} \quad \partial_y w_1 + \partial_x w_2 + \partial_x u_3\partial_y u_3 = 0 \quad \text{in } \Omega_{2,\delta}. \tag{35}$$

Combining (34) and (35), we have

$$\int_{\Omega_{2,\delta}} |e(w) + \tfrac{1}{2}\nabla u_3\otimes\nabla u_3 - I|^2 = 0.$$

On the other hand from (30) we have

$$\alpha_m h \int_{\Omega_{1,\delta}} |e(w) + \frac{1}{2}\nabla u_3 \otimes \nabla u_3 - I|^2 \lesssim \alpha_m h\delta \lesssim h\alpha_s^{2/3}$$

using (26). Thus the membrane energy on $[0,1/2]\times[0,1]$ has the desired bound:

$$\alpha_m h \int_0^{1/2}\int_0^1 |e(w) + \tfrac{1}{2}\nabla u_3 \otimes \nabla u_3 - I|^2 \, dy\, dx \lesssim h\alpha_s^{2/3}. \tag{36}$$

Step 3: The bending energy in $[0,1/2]\times[0,1]$ is

$$h^3 \int_0^{1/2}\int_0^1 |\nabla^2 u_3|^2.$$

The integrand is at most of order $a_0^{-2}$, by (30). Using the choice of $a_0$, (25), we conclude that the bending energy has the desired bound:

$$h^3 \int_0^{1/2}\int_0^1 |\nabla^2 u_3|^2 \, dy\, dx \lesssim h\alpha_s^{2/3}. \tag{37}$$

Step 4: We need the $L^2$ norms of $u_3$ and $\nabla u_3$, because we will use them to estimate the substrate energy by interpolation. The definition of $u_3$ yields

$$\int_0^{1/2}\int_0^1 |u_3|^2 \lesssim |a_0|^2 \lesssim h^2\alpha_s^{-2/3}, \tag{38}$$

and by (30) we have

$$\int_0^{1/2}\int_0^1 |\nabla u_3|^2 \lesssim 1. \tag{39}$$

It follows in particular that

$$\alpha_s \|u_3\|_{L^2([0,1/2]\times[0,1])} \|\nabla u_3\|_{L^2([0,1/2]\times[0,1])} \le h\alpha_s^{2/3}. \tag{40}$$

Step 5: We extend $(w_1, w_2, u_3)$ to $[1,2]\times[0,1]$ by setting

$$u_3(x,y) = u_3(1-x,y), \quad w_2(x,y) = w_2(1-x,y), \quad \text{and} \quad w_1(x,y) = -w_1(1-x,y),$$

when $(x,y)\in[1/2,1]\times[0,1]$. Then $\nabla_x w_1$, $\nabla_y w_2$, $|\nabla_x u_3|^2$ and $|\nabla_y u_3|^2$ are all even in $x$, while $\nabla_x w_2 + \nabla_y w_1$ and $\nabla_x u_3 \nabla_y u_3$ are both odd in $x$. Thus the membrane energy on $[0,1]^2$ is exactly twice the membrane energy on $[0,1/2]\times[0,1]$. Similarly, the bending and substrate energies are also twice their values on $[0,1/2]\times[0,1]$. We conclude that

$$\alpha_m h \int_{[0,1]^2} |e(w) + \tfrac{1}{2}\nabla u_3 \otimes \nabla u_3 - I|^2 + h^3 \int_{[0,1]^2} |\nabla^2 u_3|^2 \lesssim h\alpha_s^{2/3}.$$

Also, combining the interpolation inequality

$$\|u_3\|_{H^{1/2}} \lesssim \|u_3\|_{L^2}^{1/2} \|\nabla u_3\|_{L^2}^{1/2} \tag{41}$$

with (40) we have

$$\alpha_s \|u_3\|_{H^{1/2}}^2 \lesssim h\alpha_s^{2/3}.$$

This establishes (23), completing the proof. □

**Remark 2.** *Our construction amounts to a herringbone with just two columns. The preceding discussion focuses on the rescaled problem. In the original variables, where the membrane energy is a constant times* $\int |e(w) + \frac{1}{2}\nabla u_3 \otimes \nabla u_3 - \eta I|^2$*, the deformation in the left "column" of the herringbone is the superposition of*

*(i) a uniform in-plane shear* $(w', u_3')$ *with* $u_3' = 0$ *and* $e(w') = \begin{pmatrix} 0 & -\eta \\ -\eta & 0 \end{pmatrix}$*, and*

*(ii) a wrinkling deformation* $(w'', u_3'')$ *chosen so that* $e(w'') + \frac{1}{2}\nabla u_3'' \otimes \nabla u_3'' = \begin{pmatrix} \eta & \eta \\ \eta & \eta \end{pmatrix}$*.*

*The superposition* $w = w' + w'', u = u''$ *achieves* $e(w) + \frac{1}{2}\nabla u_3 \otimes \nabla u_3 - \eta I = 0$ *pointwise, however the average of* $e(w)$ *is not zero; rather, it is* $\begin{pmatrix} 0 & -\eta \\ -\eta & 0 \end{pmatrix}$*. The right column of the herringbone fixes this: there the deformation is a superposition of the opposite in-plane shear with a suitable wrinkling deformation, again achieving* $e(w) + \frac{1}{2}\nabla u_3 \otimes \nabla u_3 - \eta I = 0$ *pointwise, this time with average in-plane strain* $\begin{pmatrix} 0 & \eta \\ \eta & 0 \end{pmatrix}$*. By combining the two deformations in equal area fractions, the construction achieves average in-plane strain zero, permitting* $w$ *to be spatially periodic.*

# 4 The improved model

In the original physical variables $(x, y) \in [0, L]^2$, the construction of Section 3 has wrinkles of wavelength $\alpha_s^{-1/3}(h/L)L = \alpha_s^{-1/3}h$, superimposed upon an in-plane shear that oscillates on the domain-size scale $L$. We could have decreased the wavelength of the in-plane shear oscillation (at the expense of introducing additional transition layers), but there was no reason to do so, because our substrate term involved only $u_3$.

As explained in Section 1.1, to do better we must account for the substrate energy associated with $w$. Therefore we turn now to the functional $\mathcal{E}^*$, defined by (6). Nondimensionalizing as in Section 1.3, we have

$$\mathcal{E}^* = \eta L \Big\{ \tilde{\alpha}_m \tilde{h} \int_{[0,1]^2} |e(\tilde{w}) + \tfrac{1}{2}\nabla \tilde{u}_3 \otimes \nabla \tilde{u}_3 - I|^2 + \tilde{h}^3 \int_{[0,1]^2} |\nabla^2 \tilde{u}_3|^2 + \alpha_s \|\tilde{u}_3\|_{H^{1/2}}^2 + \alpha_s \eta \|\tilde{w}\|_{H^{1/2}}^2 \Big\}. \tag{42}$$

with $\tilde{\alpha}_m = \alpha_m \eta$ and $\tilde{h} = h/L$. As in (16), the expression in brackets on the right has membrane and bending terms identical to those of $\mathcal{E}$ with $\eta$ replaced by 1, $h$ replaced by $\tilde{h}$, and $\alpha_m$ replaced by $\tilde{\alpha}_m$. The substrate term associated with $u_3$ is also identical to that

of (16). The only difference from (16) is the presence of the substrate energy associated with $w$ – which has coefficient $\alpha_s\eta$ rather than $\alpha_s$. Since $\eta$ is small, it is tempting to ignore this term, i.e. to study $\mathcal{E}$ rather than $\mathcal{E}^*$. However it is the substrate energy associated to $w$ that sets the length scale on which the wrinkling direction oscillates.

Our plan for proving Theorem 3 is simple: we proceed exactly as for Theorem 2, except that we let the direction of wrinkling oscillate on scale $\ell$ rather than on the scale of the domain. Optimization of $\ell$ identifies the optimal herringbone pattern. The conditions in (13) identify the regime where this pattern makes sense (the optimal $\ell$ is larger than the scale of the wrinkling and smaller than that of the period cell) and its energy has the same scaling as our lower bound.

*Proof of Theorem 3.* Since the argument is an extension of the one for Theorem 2 we shall work with the nondimensionalized problem, whose period cell is $[0,1]^2$. We shall show that if

$$\tilde{\alpha}_m \geq \alpha_s^{2/3}, \quad \tilde{\alpha}_m \alpha_s^{-4/3} \eta^{-1} \tilde{h}^2 \leq 1, \quad \text{and} \quad \eta \leq \tilde{\alpha}_m^{-1} \alpha_s^{2/3} \tag{43}$$

then there exists a periodic herringbone-type deformation $(\tilde{w}_1, \tilde{w}_2, \tilde{u}_3)$ on $[0,1]^2$, involving wrinkles with wavelength on scale $\tilde{h}\alpha_s^{-1/3}$ whose direction oscillates on the longer scale $(\tilde{h}\alpha_s^{-1/3})\tilde{\alpha}_m^{1/2}\alpha_s^{-1/3}\eta^{-1/2}$ such that

$$\tilde{\alpha}_m \tilde{h} \int_{[0,1]^2} \left| e(\tilde{w}) + \tfrac{1}{2}\nabla \tilde{u}_3 \otimes \nabla \tilde{u}_3 - I \right|^2 + \tilde{h}^3 \int_{[0,1]^2} |\nabla^2 \tilde{u}_3|^2 + \alpha_s \|\tilde{u}_3\|_{H^{1/2}}^2 + \alpha_s \eta \|\tilde{w}\|_{H^{1/2}}^2 \lesssim \tilde{h}\alpha_s^{2/3}. \tag{44}$$

Theorem 3 follows immediately from this assertion and (42).

The remainder of this section addresses (44). To simplify the notation stay parallel to the proof of Theorem 2, we henceforth *drop all the tildes.*

The proof of Theorem 2 used wrinkling on scale $a_0 \sim h\alpha_s^{-1/3}$, with normal $(1,1)$ on the left half of the cell and normal $(-1,1)$ on the right half of the cell, and with a transition layer of width $\delta$ where the direction of wrinkling reverses. The precise value of $\delta$ was unimportant provided that $\delta \gtrsim a_0$.

Here we proceed similarly, except that we take the scale on which the wrinkling reverses to be $\ell$, with $(2\ell)^{-1}$ a positive integer. Since there is no advantage to taking $\delta$ large, we take $\delta \sim a_0$.

To be more explicit about the construction:

- For $x$ between $\delta$ and $\ell - \delta$, $(w_1, w_2, u_3)$ is exactly as it was in the proof of Theorem 2 between $\delta$ and $1/2 - \delta$.

- For $x$ in $[0, \delta]$ or $[\ell - \delta, \ell]$, we use a cutoff function exactly as in Theorem 2, except for replacing $1/2$ by $\ell$. Thus $w_1 = 0$ and $u_3 = 0$ near $x = 0$ and near $x = \ell$, while $w_2 = -2x$ near $x = 0$ and near $x = \ell$.

- Having defined the deformation in $[0,\ell]$, we now extend it to $[\ell,2\ell]$ by reflection as in the proof of Theorem 2, using even reflection for $u_3$ and $w_2$ and odd reflection for $w_1$, i.e.

$$u_3(x) = u_3(2\ell - x), \quad w_2(x) = w_2(2\ell - x), \quad w_1(x) = -w_1(2\ell - x) \quad \text{for } \ell < x < 2\ell.$$

- The resulting deformation is a periodic function of $x \in [0,2\ell]$. We may therefore extend it to all $x \in [0,1]$ by periodicity (using the hypothesis that $(2\ell)^{-1}$ is an integer).

For this construction to make sense, the boundary layers must not touch one another. Remembering the choice $\delta \sim a_0$, this requires that $a_0 \lesssim \ell$.

The membrane energy is now

$$\alpha_m h \int_{[0,1]^2} \left| e(w) + \tfrac{1}{2}\nabla u_3 \otimes \nabla u_3 - I \right|^2 \lesssim \alpha_m h a_0 \ell^{-1},$$

since the integrand vanishes except in the $1/\ell$ "transition layers," each having width $2\delta \sim a_0$, where the integrand is of order 1.

The estimates of the bending energy and the substrate energy associated with $u_3$ are exactly as in the proof of Theorem 2:

$$h^3 \int_{[0,1]^2} |\nabla^2 u_3|^2 \lesssim h^3 a_0^{-2}, \quad \alpha_s \|u_3\|_{H^{1/2}}^2 \lesssim \alpha_s a_0,$$

since $|u_3| \lesssim a_0$, $|\nabla u_3| \lesssim 1$, and $|\nabla^2 u_3| \lesssim a_0^{-1}$ pointwise.

To estimate the substrate energy of $w$, we observe that $w_2$ is a piecewise-linear sawtooth function of $x$ with wrinkles superimposed. The wrinkles have amplitude $\sim a_0$ and slope $\sim 1$; the sawtooth has amplitude $\sim \ell$ and slope $\sim 1$. Since $a_0 \lesssim \ell$, the sawtooth dominates in the estimation of the $L^2$ norm, giving $\|w_2\|_{L^2} \sim \ell$. The other component $w_1$ is different: it consists only of wrinkles, and its estimation is similar to that of $u_3$: $|w_1| \lesssim a_0$ and $|\nabla w_1| \lesssim 1$, whence in particular $\|w_1\|_{L^2} \lesssim a_0$. Since $a_0 \lesssim \ell$ it follows that $\|w\|_{L^2} \lesssim \ell$; therefore, using the interpolation inequality (41),

$$\eta\alpha_s \|w\|_{H^{1/2}}^2 \lesssim \eta\alpha_s \|w\|_{L^2} \|\nabla w\|_{L^2} \lesssim \eta\alpha_s \ell.$$

Adding the preceding estimates, we get an upper bound for the total energy:

$$\left(h^3 a_0^{-2} + \alpha_s a_0\right) + \left(\alpha_m h a_0 \ell^{-1} + \eta\alpha_s \ell\right)$$

The first term is optimally of order $h\alpha_s^{2/3}$, achieved when $a_0 \sim h\alpha_s^{-1/3}$. The second term is optimally of order

$$(\alpha_m h a_0)^{1/2} (\eta\alpha_s)^{1/2}$$

by the arithmetic mean – geometric mean inequality, achieved when

$$\ell^2 \sim \frac{\alpha_m h a_0}{\eta\alpha_s}. \tag{45}$$

Using $a_0 \sim h\alpha_s^{-1/3}$, one verifies that

$$\ell \sim a_0 \left( \frac{\alpha_m}{\eta \alpha_s^{2/3}} \right)^{1/2}; \tag{46}$$

Notice that $a_0 \lesssim \ell$, as a consequence of the first condition in (43) (using also that $\eta \leq 1$). The third condition in (43) assures that the energy terms involving $\ell$ are subdominant, since

$$(\alpha_m h a_0)^{1/2} (\eta \alpha_s)^{1/2} \lesssim h \alpha_s^{2/3} \Leftrightarrow \eta \lesssim \alpha_m^{-1} \alpha_s^{2/3}.$$

For the construction to be feasible we need $\ell \lesssim 1$; this is assured by the second condition in (43). □

**Remark 3.** *Since the energy terms involving $\ell$ are subdominant, the system has little incentive to use the optimal value of $\ell$. This is consistent with the numerical and experimental observation that while the length scale of the wrinkling is sharply determined, the scale on which the wrinkling oscillates is much less sharply determined [12, 22, 34].*

# References


[1] B. Audoly and A. Boudaoud, *Buckling of a stiff film bound to a compliant substrate–Part I: Formulation, linear stability of cylindrical patterns, secondary bifurcations*, J. Mech. Phys. Solids **56** (2008), 2401–2421.

[2] _____, *Buckling of a stiff film bound to a compliant substrate–Part II: A global scenario for the formation of herringbone pattern*, J. Mech. Phys. Solids **56** (2008), 2422–2443.

[3] _____, *Buckling of a stiff film bound to a compliant substrate–Part III: Herringbone solutions at large buckling parameter*, J. Mech. Phys. Solids **56** (2008), 2444–2458.

[4] B. Audoly and Y. Pomeau, *Elasticity and Geometry: From Hair Curls to the Nonlinear Response of Shells*, Oxford University Press (2010).

[5] P. Bella and R. V. Kohn, *Wrinkles as the result of compressive stresses in an annular thin film*, to appear in Comm. Pure Appl. Math.

[6] H. Ben Belgacem, S. Conti, A. DeSimone, and S. Müller, *Rigorous bounds for the Föppl–von Karman theory of isotropically compressed plates*, J. Nonlinear Sci. **10** (2000), 661–683.

[7] _____, *Energy scaling of compressed elastic films – three dimensional elasticity and reduced theories*, Arch. Rational Mech. Anal. **164** (2002), 1–37.

[8] N. Bowden, S. Brittain, A. G. Evans, J. W. Hutchinson, and G. M. Whitesides, *Spontaneous formation of ordered structures in thin films of metals supported on an elastomeric polymer*, Nature **393** (1998), 146–149.

[9] D. Breid and A. J. Crosby, *Surface wrinkling behavior of finite circular plates*, Soft Matter **5** (2009), 425–431.

[10] S. Cai, D. Breid, A. J. Crosby, Z. Suo, and J. W. Hutchinson, *Periodic patterns and energy states of buckled films on compliant substrates*, J. Mech. Phys. Solids **59** (2011), 1094–1114.

[11] X. Chen and J. W. Hutchinson, *Herringbone buckling patterns of compressed thin films on compliant substrates*, J. Appl. Mech. **71** (2004), 597–603.

[12] _____, *A family of herringbone patterns in thin films*, Scripta Materialia **50** (2004), 797–801.

[13] R. Choksi, R. V. Kohn, and F. Otto, *Domain branching in uniaxial ferromagnets: a scaling law for the minimum energy*, Comm. Math. Phys. **201** (1999), 61–79.

[14] R. Choksi, S. Conti, R. V. Kohn, and F. Otto, *Ground state energy scaling laws during the onset and destruction of the intermediate state in a type-I superconductor*, Comm. Pure Appl. Math. **61** (2008), 595–626.

[15] S. Conti, *Branched microstructures: scaling and asymptotic self-similarity*, Comm. Pure Appl. Math. **53** (2000), 1448–1474.

[16] S. Conti and F. Maggi, *Confining thin elastic sheets and folding paper*, Arch. Rat. Mech. Anal. **187** (2008), 1–48.

[17] B. Davidovitch, R. D. Schroll, D. Vella, M. Addia-Bedia, and E. Cerda, *Prototypical model for tensional wrinkling in thin sheets*, Proc. Natl. Acad. Sci. **108** (2011), 18227–18232.

[18] K. Efimenko, M. Rackaitis, E. Manias, A. Vaziri, L. Mahadevan, and J. Genzer, *Nested self-similar wrinkling patterns in skins*, Nature Materials **4** (2005), 293–297.

[19] G. Friesecke, R. D. James, and S. Müller, *A hierarchy of plate models derived from nonlinear elasticity by gamma-convergence*, Arch. Rational Mech. Anal. **180** (2006), 183–236.

[20] J. Genzer and J. Groenewold, *Soft matter with hard skin: From skin wrinkles to templating and material characterization*, Soft Matter **2** (2006), 310–323.

[21] G. Gioia and M. Ortiz, *Delamination of compressed thin films*, Adv. Appl. Mech. **33** (1997), 119–192.

[22] Z. Huang, W. Hong, and Z. Suo, *Evolution of wrinkles in hard films on soft substrates*, Phys. Rev. E **70** (2004), 030601(R).

[23] _____, *Nonlinear analyses of wrinkles in a film bonded to a compliant substrate*, J. Mech. Phys. Solids **53** (2005), 2101–2118.

[24] R. Huang and S. H. Im, *Dynamics of wrinkle growth and coarsening in stressed thin films*, Phys Rev E **74** (2006), 026214.

[25] S. H. Im and R. Huang, *Wrinkle patterns of anisotropic crystal films on viscoelastic substrates*, J. Mech. Phys. Solids **56** (2008), 3315–3330.

[26] E. Jagla, *Modeling the buckling and delamination of thin films*, Phys. Rev. B **75** (2007), 085405.

[27] W. Jin and P. Sternberg, *Energy estimates for the von Karman model of thin-film blistering*, J. Math. Phys. **42** (2001), 192–199.

[28] R. V. Kohn and S. Müller, *Surface energy and microstructure in coherent phase transitions*, Comm. Pure Appl. Math. **47** (1994), 405–435.

[29] R. V. Kohn and H. Nguyen, in preparation.

[30] P.-C. Lin and S. Yang, *Spontaneous formation of one-dimensional ripples in transit to highly ordered two-dimensional herringbone structures through sequential and unequal biaxial mechanical stretching*, Appl. Phys. Lett. **90** (2007), 241903.

[31] A. E. Lobkovsky and T. A. Witten, *Properties of Ridges in Elastic Membranes*, Phys. Rev. E **55** (1997), 1577–1589.

[32] L. Mahadevan and S. Rica, *Self-organized origami*, Science **307** (2005), 1740.

[33] Y. Ni, L. He, and Q. Liu, *Modeling kinetics of diffusion-controlled surface wrinkles*, Phys. Rev. E **84** (2011), 051604

[34] J. Song, H. Jiang, W. M. Choi, D. Y. Khang, Y. Huang, and J. A. Rogers, *An analytical study of two-dimensional buckling of thin films on compliant substrates*, J. Appl. Phys. **103** (2008), 014303.

[35] J. Song, H. Jiang, Z. J. Liu, D. Y. Khang, Y. Huang, J. A. Rogers, C. Lu, and C. G. Koh, *Buckling of a stiff thin film on a compliant substrate in large deformation*, Intl. J. Solids Struct. **45** (2008), 3107–3121.

[36] J. Song, H. Jiang, Y. Huang, and J. A. Rogers, *Mechanics of stretchable inorganic electronic materials*, J. Vac. Sci. Technol A **27** (2009), 1107–1125.

[37] E. Sultan and A. Boudaoud, *The buckling of a swollen thin gel layer bound to a compliant substrate*, J. Appl. Mech. **75** (2008), 051002.

[38] H. Vandeparre and P. Damman, *Wrinkling of stimuloresponsive surfaces: Mechanical instability coupled to diffusion*, Phys. Rev. Lett **101** (2008), 124301.

[39] S. C. Venkataramani, *Lower bounds for the energy in a crumpled elastic sheet – A minimal ridge*, Nonlinearity **17** (2004), 301–312.

[40] T. A. Witten, *Stress focusing in elastic sheets*, Rev. Mod. Phys. **79** (2007), 643–675.

[41] J. Yin, X. Chen, and I. Sheinman, *Anisotropic buckling patterns in spheroidal film/substrate systems and their implications in some natural and biological systems*, J. Mech. Phys. Solids **57** (2009), 1470–1484.